

SCIENTIFIC REPORTS



OPEN

Prophylactic Active Tau Immunization Leads to Sustained Reduction in Both Tau and Amyloid- β Pathologies in 3xTg Mice

Hameetha Rajamohamedsait¹, Suhail Rasool¹, Wajitha Rajamohamedsait¹, Yan Lin¹ & Einar M. Sigurdsson^{1,2}

Amyloid- β (A β) and tau pathologies are intertwined in Alzheimer's disease, and various immunotherapies targeting these hallmarks are in clinical trials. To determine if tau pathology influences A β burden and to assess prophylactic benefits, 3xTg and wild-type mice received tau immunization from 2–6 months of age. The mice developed a high IgG titer that was maintained at 22 months of age. Pronounced tau and A β pathologies were primarily detected in the subiculum/CA1 region, which was therefore the focus of analysis. The therapy reduced histopathological tau aggregates by 70–74% overall (68% in males and 78–86% in females), compared to 3xTg controls. Likewise, western blot analysis revealed a 41% clearance of soluble tau (38–76% in males and 48% in females) and 42–47% clearance of insoluble tau (47–58% in males and 49% in females) in the immunized mice. Furthermore, A β burden was reduced by 84% overall (61% in males and 97% in females). These benefits were associated with reductions in microgliosis and microhemorrhages. In summary, prophylactic tau immunization not only prevents tau pathology but also A β deposition and related pathologies in a sustained manner, indicating that tau pathology can promote A β deposition, and that a short immunization regimen can have a long-lasting beneficial effect.

Alzheimer's disease (AD) is characterized by accumulation of extracellular amyloid- β (A β) plaques, intracellular neurofibrillary tangles (NFT), and extensive synaptic loss leading to progressive cognitive impairment and eventually dementia. NFT are primarily composed of filaments of aggregated hyperphosphorylated tau protein¹. Extensive work by numerous investigators suggests that A β pathology may lead to tau pathology². However, it is interesting to note that reanalysis of a large number of human AD and control brains of various ages with phospho-specific tau antibodies revealed that phospho-tau immunoreactivity is generally detected in control brains prior to A β deposition³. This unexpected finding suggests that tau pathology may precede A β pathology in AD, at least in certain individuals, although it is of course unclear if these subjects would ever have developed the disease. Importantly, A β plaque clearance has had limited effect on tau pathology in the A β immunotherapy trials (for review see⁴), which emphasizes the need for therapy that specifically targets this other major hallmark of the disease. Numerous reports by us and others have shown the feasibility of tau immunotherapy^{5–35}, and several clinical trials have been initiated (for review see³⁶). However, all these studies were conducted in mice or related culture models that have only tau pathology but no A β pathology. Tau antibody immunization in A β plaque models has been reported to improve cognition and clear certain A β species while increasing A β plaque burden³⁷, or when using a different tau antibody in a different A β model provided no cognitive benefits and increased mortality³⁸. A few prior studies have reported toxic effects of active tau immunization in mice when very strong adjuvants are being used^{39,40}.

¹Departments of Neuroscience and Physiology, New York University School of Medicine, 550 First Avenue, New York, NY, 10016, United States. ²Departments of Psychiatry, New York University School of Medicine, 550 First Avenue, New York, NY, 10016, United States. Correspondence and requests for materials should be addressed to E.M.S. (email: enar.sigurdsson@nyumc.org)

	Start of Study	End of Study -Tissue Analysis
3xTg Control	19 (9 M + 10 F)	16 (6 M + 10 F)
3xTg Phos-tau	24 (13 M + 11 F)	24 (13 M + 11 F)
WT Control	14 (7 M + 7 F)	10 (4 M + 6 F)
WT Phos-tau	17 (8 M + 9 F)	15 (7 M + 8 F)

Table 1. Number of mice of each gender at the beginning and end of the study. Only a few mice died during the study, and most of those were in the control group. None of the 3xTg treated mice died. M = male, F = female.

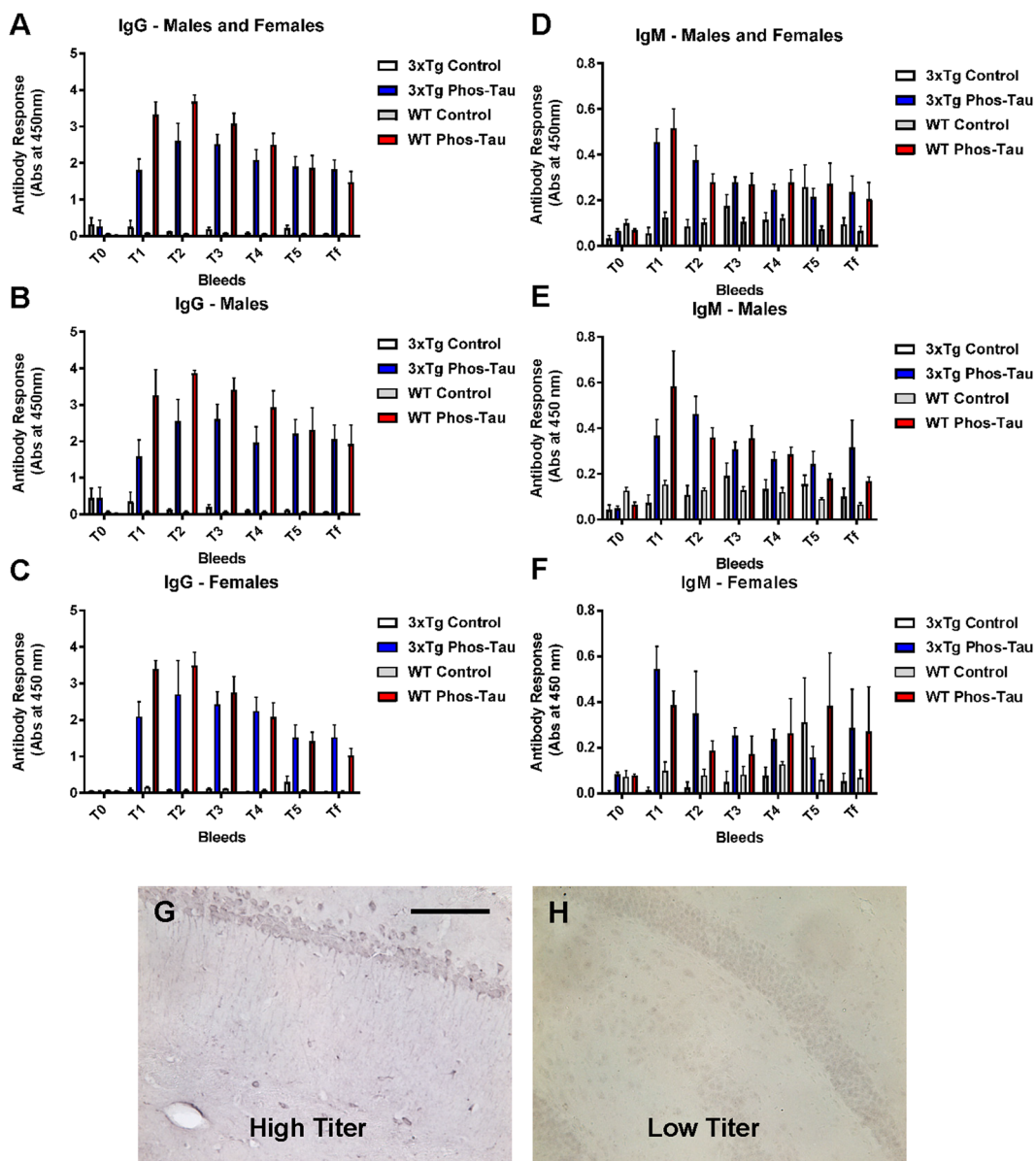


Figure 1. The tau immunogen Tau379–408[P-Ser396, 404] elicits a robust and sustained antibody response. (A–C) IgG response towards the immunogen was strong and long-lasting, and comparable in males vs. females. It was strong at T1 (1 week after the 3rd immunization), peaked at T2 (2 months after the 4th and last immunization) and remained strong thereafter (T3–Tf: 5, 8, 11, and 16 months after the 4th immunization). Higher IgG levels were detected in wt mice compared to 3xTg mice. (D–F) IgM response was not as strong as the IgG response but showed a similar pattern as the IgG response except that the IgM response was comparable in the wt vs. the 3xTg mice. (G,H) Plasma (1:100) obtained from a high titer mouse at the end of the study (Tf) stained tau aggregates in a control 3xTg mouse, whereas plasma from a low titer control mouse did not. Scale bar: 125 μ m.

PHF1

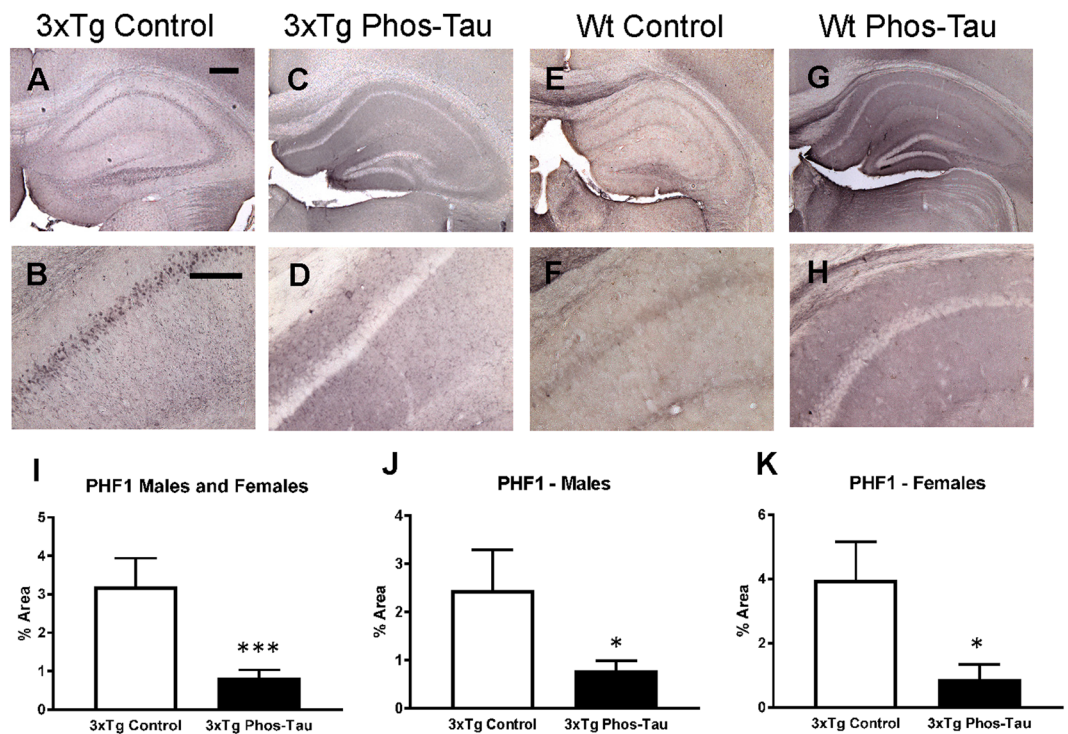


Figure 2. Tau immunization prevents phospho-tau histopathology. (A–D) PHF1 immunostaining revealed extensive tau pathology in the hippocampus (A: 5X objective, B: 20X objective) of 3xTg mice, that was greatly reduced in immunized mice (C,D). (E–H) Only background staining was seen in the wt mice. (I–K) Quantitative analysis of the PHF1 staining revealed significant reduction in tau aggregates in the combined group (I: 74%, $p = 0.0008$) as well as in males (J: 68%, $p = 0.0437$) and females (K: 78%, $p = 0.0120$) analyzed separately. Scale bar: 250 μm (A), 125 μm (B). * $p < 0.05$; *** $p < 0.001$ compared to 3xTg control. See text for exact p-values.

One of the few models with both $A\beta$ and tau deposits, is the triple transgenic (3xTg) mouse model, which harbors a presenilin 1 mutation (PS1/M146V) knock in allele, as well as the Swedish mutation of the amyloid precursor protein (APP^{Swe}), and tau P301L mutation transgenes⁴¹. The PS1 and APP mutations individually cause familial AD and the tau mutation leads to frontotemporal dementia, which is an $A\beta$ negative tauopathy. The 3xTg mice develop age-dependent and region-specific $A\beta$ and tau deposits that mimic the disease progression in humans. They have previously received $A\beta$ immunotherapy, which cleared $A\beta$ plaques and rescued early but not late hyperphosphorylated tau aggregates⁴². More recently, a couple of studies have reported on the effect of tau antibodies on tau and $A\beta$ burden in 3xTg mice^{43,44}. A single injection of AT8, a phospho-tau antibody was shown to transiently reduce tau pathology without affecting $A\beta$ pathology⁴³. More recently, multiple injections of another tau antibody acutely reduced tau and $A\beta$ pathology in their early stages⁴⁴. Here, we report that immunization of this 3xTg model with Tau379–408[P-Ser396, 404] from 3–6 months of age, with animals killed at 22 months for analysis, resulted in a robust tau antibody response and long-term clearance of not only tau aggregates but also associated $A\beta$ plaques.

Materials and Methods

Peptides. Phosphorylated tau peptide, Tau379–408[P-Ser396,404], was synthesized and purified at the Keck facility (Yale University) as described previously⁵.

Transgenic Mice. The treatment was performed in 3xTg transgenic mice expressing knock-in mutation PS1/M146V combined with APP/K670N, M671L and MAPT/P301L transgenes⁴¹. A breeding pair of homozygous mice and another pair of wild-type (wt) mice of the same mixed strain background (C57BL6/129 SVJ) were graciously donated by Frank LaFerla (University of California at Irvine). These mice develop plaque and tangle pathology in AD relevant brain regions (hippocampus, cortex and amygdala). Wt mice from the same background were used as a control. The mice were housed in Association for Assessment and Accreditation of Laboratory Animal Care (AAALAC) approved facilities. All mouse care and experimental procedures were compliant with guidelines of animal experimentation and were approved by the Institutional Animal Care and Use committee at New York University School of Medicine.

Vaccine Administration. At the start of the study, the 3xTg and wt mice were split into treatment groups that received the tau vaccine and control groups that received adjuvant alone (Table 1). The immunogen Tau

MC1

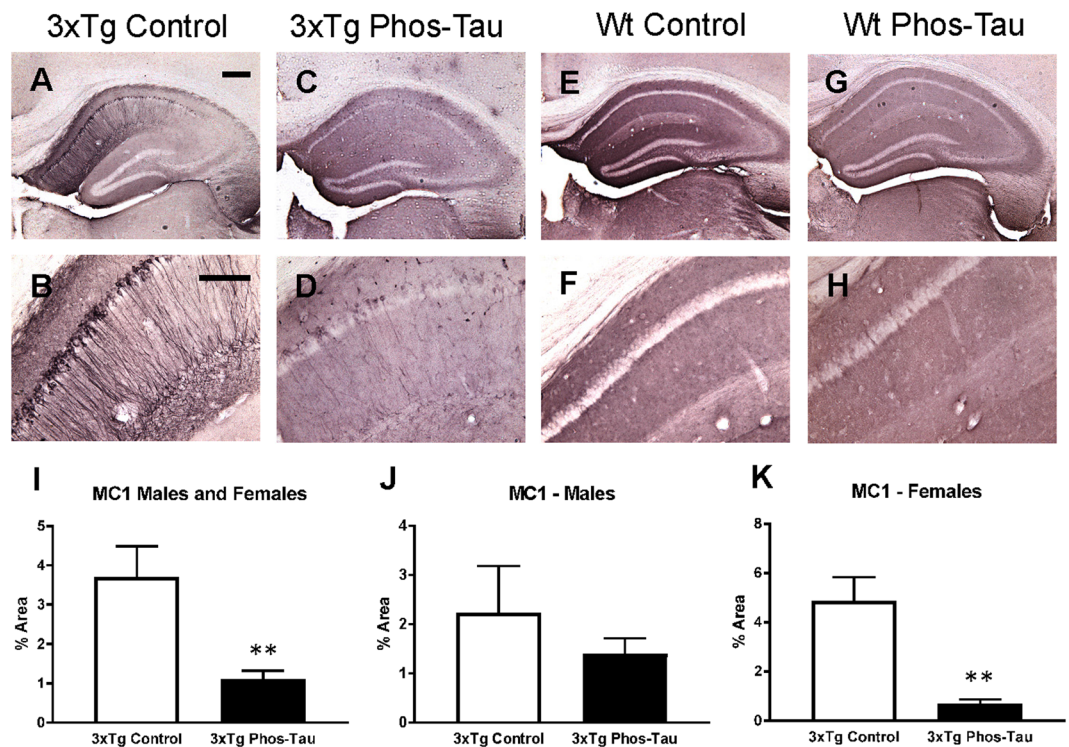


Figure 3. Tau immunization prevents conformational tau histopathology. (A–D) MC1 immunostaining revealed extensive tau pathology in the hippocampus (A: 5X objective, B: 20X objective) of 3xTg mice, that was greatly decreased in immunized 3xTg mice (C–D). (E–H) Only background staining was seen in the wt mice. (I–K) Quantitative analysis of the MC1 staining revealed significant reduction in tau aggregates in the combined group (I: 70%, $p = 0.0057$) as well as in females (K: 86%, $p = 0.0070$). Scale bar: 250 μm (A), 125 μm (B). ** $p < 0.01$ compared to 3xTg control. See text for exact p-values.

379–408 [P-Ser396, 404] was added to Adju-Phos adjuvant (Brenntag Biosector, Denmark) (1 mg/mL) and mixed overnight at 4 °C the day before injection for the peptide to adsorb onto the aluminum phosphate particles. The vaccine was injected subcutaneously (100 μl) with a second injection administered two weeks later and subsequent injections monthly thereafter. The treatment period was from 3–6 months of age (four injections). The mice were bled before the first immunization (T0) and then periodically thereafter to monitor their tau antibody response (T1: 1 week after the 3rd immunization; T2–T5: 2, 5, 8 and 11 months after the 4th immunization, respectively; T6: 16 months after the 4th immunization). At 22 months, their brains were extracted for analyses. The mice went through several behavioral tests in the two months prior to killing. At the end of study, a few mice had died in each of the four groups except in the immunized 3xTg groups, in which all the mice survived the experimental period (Table 1). Upon western blot analysis, 3 Tg mice (2 control males and 1 control female) were eliminated from the study because they did not express human tau, although the transgene was present. We have observed this at a similar rate in other Tg tauopathy models over the years. These three mice are not included in Table 1 or in any of the analyses.

Behavior. Each instrument was wiped clean with 30% ethanol between animals.

Locomotor activity. A circular open field activity chamber (70 cm in diameter) was used to measure exploratory locomotor activity over 15 min⁴⁵. A camera placed above the field recorded animal movements (San Diego Instruments). Measured parameters were distance traveled (in centimeters), mean resting time, and velocity [mean (V_{mean}) and maximum (V_{max})] of the mouse.

Traverse beam. This test measures balance, motor coordination and function integration⁴⁵. Mice were evaluated by examining their ability to traverse a narrow beam to enter a goal box. The animals were placed on a wooden beam (1.1 cm wide, 50.8 cm long) that was suspended 30 cm above a soft foam cushion by two identical columns. At each end of the beam was attached a shaded goal box. Habituation consisted of placing the mouse on the middle of the beam for 60 s. Subsequently, in four successive trials, the number of foot slips before falling or reaching the goal box was recorded for each mouse. Errors were defined as foot slips and their numbers counted. A mouse that fell off the beam, was placed back on it at the location it fell from.

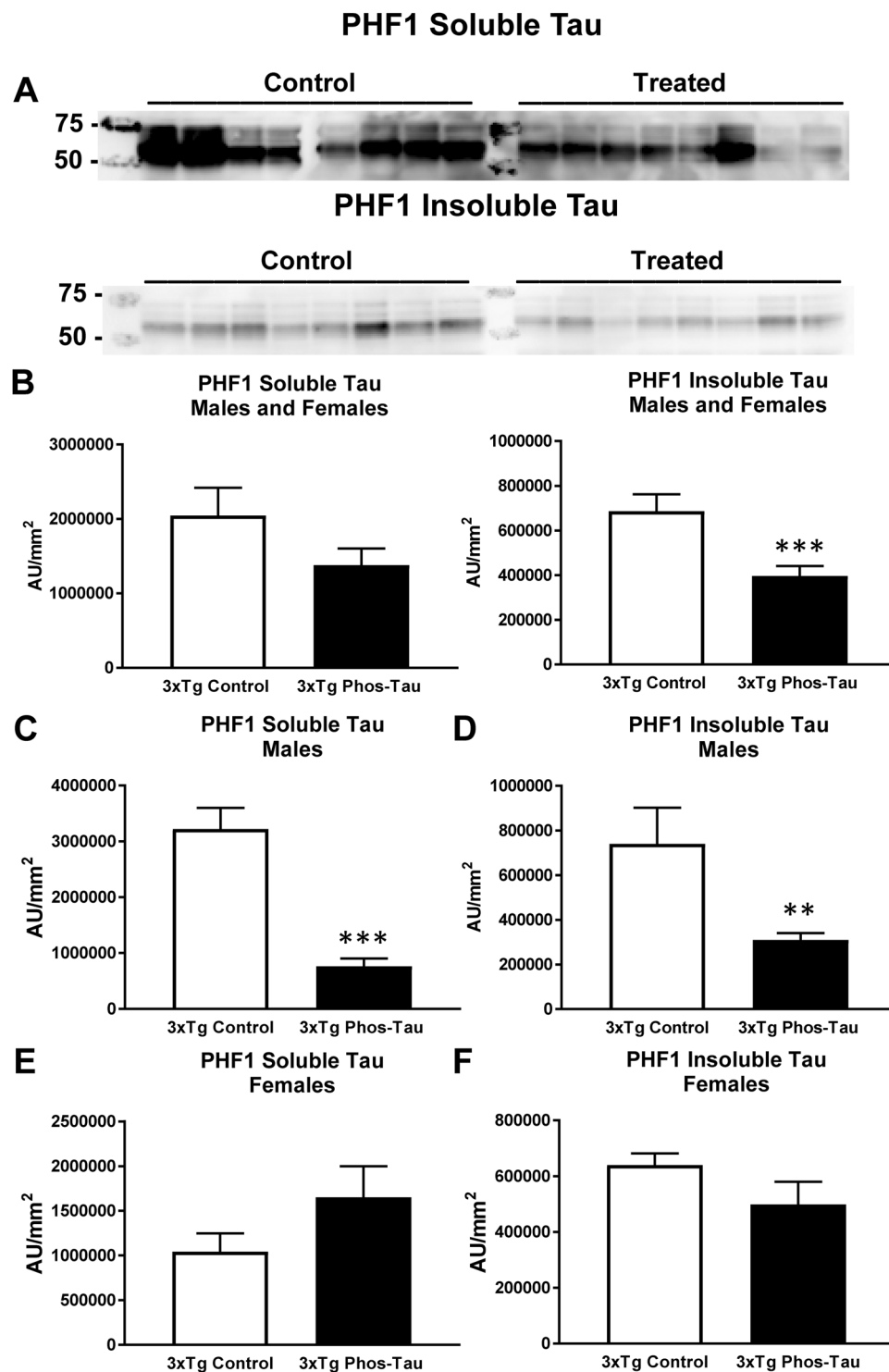


Figure 5. Tau immunization reduces soluble and insoluble phospho-tau protein. (A,B) Representative blots are shown in A. Western blot analysis revealed that insoluble PHF1-reactive human tau was decreased in the immunized 3xTg mice (42%, $p = 0.0003$). (C,D) Both soluble (76%, $p = 0.0001$) and insoluble tau (58%, $p = 0.0018$) were decreased in the males but not in the females (E,F). ** $p < 0.01$; *** $p < 0.001$ compared to 3xTg control. See text for exact p -values.

Rotarod. This test was conducted to measure potential differences in forelimb and hindlimb motor coordination and balance without a practice confound (ref.⁴⁵ Rotarod 7650 accelerating model; Ugo Basile). Habituation consisted of two trial training sessions to allow the animals to perform at a baseline level. Subsequently, the mice went through three test trials, with 15 min break between sessions. The rotarod was set 1.0 rpm and was gradually

6E10 + 4G8

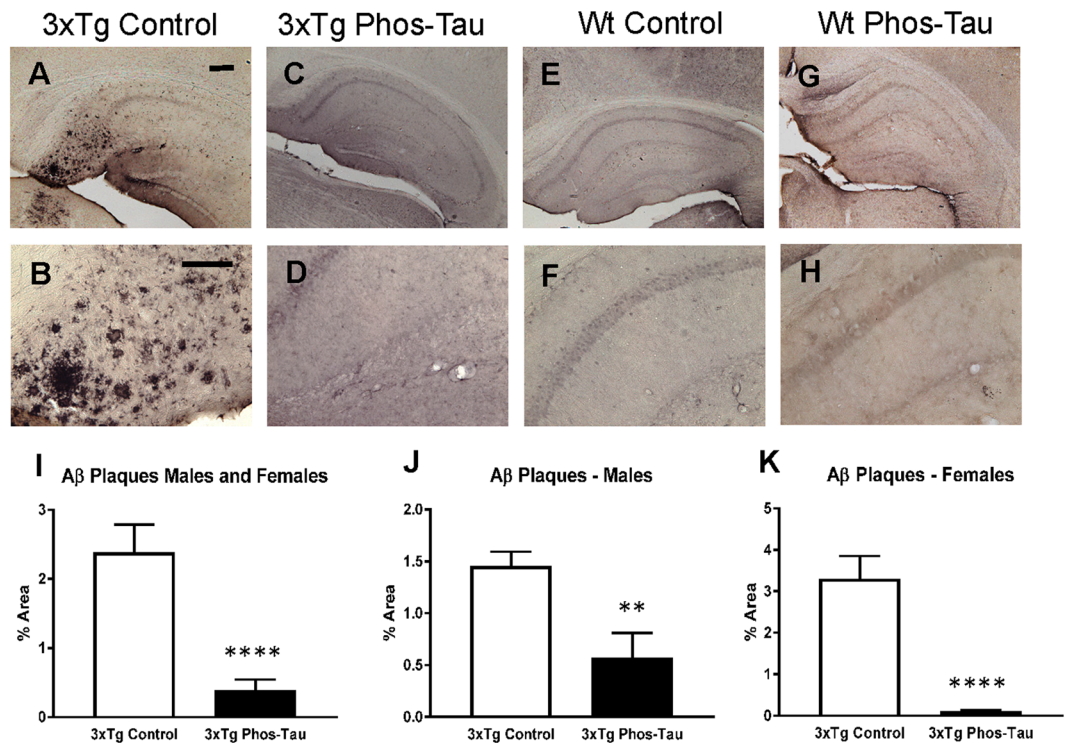


Figure 6. Tau immunization diminishes A β burden. (A–D) A β immunostaining revealed extensive A β plaque burden in subiculum region of the hippocampus (A: 5X objective, B: 20X objective) of 3xTg mice, that was greatly reduced in immunized mice (C,D). (E–H) Only background staining was seen in the wt mice. (I–K) Quantitative analysis of the A β staining revealed significant reduction in A β plaque burden in the combined group (I: 84%, $p < 0.0001$) as well as in males (J: 61%, $p = 0.0033$) and females (K: 97%, $p = 0.0001$) analyzed separately. Scale bar: 250 μ m (A), 125 μ m (B). ** $p < 0.01$; **** $p < 0.0001$ compared to 3xTg control. See text for exact p-values.

raised every 30 s until the mouse fell off or inverted (by clinging) from the rotating rod. The rpm at that point was recorded. To prevent injury, a soft foam cushion was beneath the rod.

Cognitive Tests. Before each test, the mice were adapted to the room with lights on for 15 min.

Radial arm maze. An eight-arm radial maze with a water well at the end of each arm was used to evaluate spatial learning⁴⁵. Guillotine doors made from clear Plexiglas and operated by a remote pulley system, controlled access to the arms from the central circle from which the mouse entered and exited the maze. Following adaptation for 3–4 days, water-restricted mice (2 h daily access to water) went through one training session per day for ten consecutive days. In each session, all the arms of the maze were baited with saccharine flavored water, and the mouse was allowed to enter and explore all arms until the eight sugar rewards had been consumed. Spatial learning was assessed by recording the number of errors (entries to previously visited arms) and the time needed to complete each session.

Closed field symmetrical maze. This maze consists of a rectangular field (63.5 cm square with 9 cm high walls divided into 36, 9.5 cm squares) that is covered by a clear Plexiglas top. Two boxes (each 15 \times 20 \times 9 cm), for the mice to enter or exit are situated at diagonal corners of the maze⁴⁵. This symmetrical maze⁴⁶ is based on the Hebb-Williams⁴⁷ and Rabinovitch-Rosvold⁴⁸ tests. Briefly, the key difference is that each end compartment serves as both a start box and a goal box, and the mouse navigates in opposite direction on alternate trials. An advantage of this setup is that it eliminates intertrial handling, which reduces animal stress and thereby gives more reliable data. The barriers are positioned symmetrically in the maze, so that the mouse faces the same turns going in either direction within a given setup. Before testing, the mice were adapted to a water restriction schedule, with 2 h daily access to water. Habituation consisted of two adaptation sessions before the first testing period. In the first such session, all the mice had access to saccharine flavored water in the goal box for 10 min. In the second adaptation session, the mouse was put in the start chamber and allowed to explore the field and enter the goal box, which contained saccharin water reward (0.05 mL). When the mice were consistently traveling between the start and goal boxes, they went through three practice sessions on simple navigational problems, in which one or two barriers were positioned in different regions of the maze to prevent direct route to the goal box. Formal testing

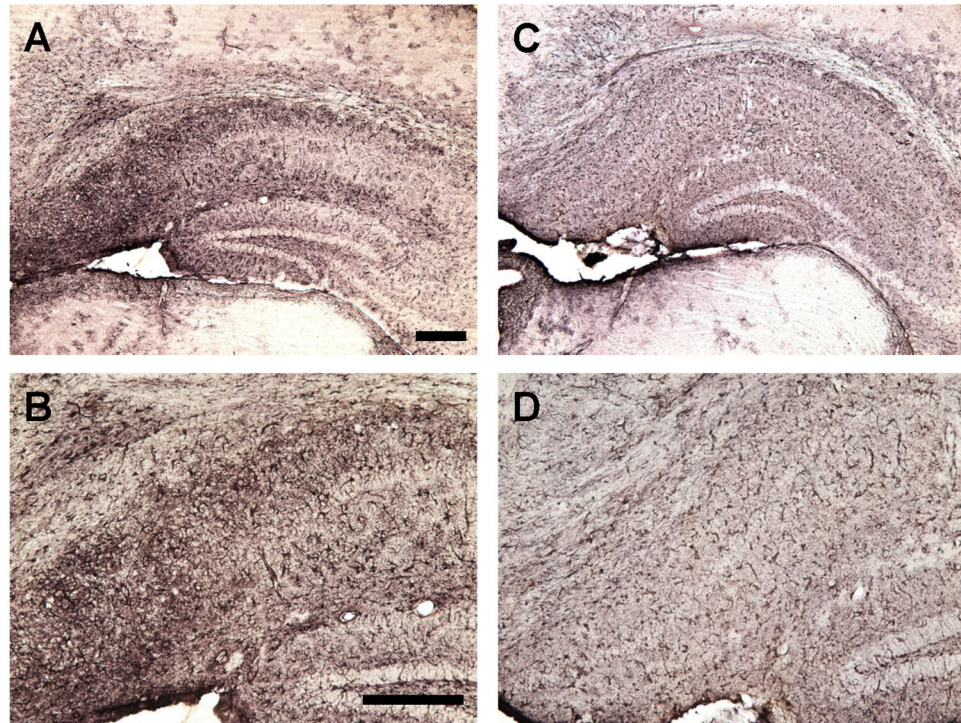


Figure 7. 3xTg mice have more astrogliosis than wt mice. (A–D) GFAP immunostaining revealed extensive astrogliosis in subiculum region of the hippocampus (A: 5X objective, B: 10X objective) of 3xTg mice, that was much less in WT mice (C,D). Scale bar: 250 μ m.

consisted of three problems of varying difficulty, starting with the easiest one and ending with the most difficult one. The mice tackled one problem per day and the mice went through five trials to solve it with an inter-trial interval of 2 min. Their performance was scored by the same person for the number of errors (i.e. entries and reentries into designated error zones) and time to complete each trial.

Antibody Response. The antibody response was determined in a 1:200 dilution of plasma using an ELISA assay as detailed previously^{49,50}, in which the immunogen was coated on to microtiter wells (Immulon 2HB, Thermo Electron). The binding of plasma antibodies was detected by a goat anti-mouse IgG or IgM linked to a horseradish peroxidase (Pierce), with the enzyme catalyzing a color reaction in the substrate (tetramethyl benzidine; Pierce).

Tissue Processing and Histology. After the behavioral testing, the mice were deeply anesthetized with ketamine/xylazine (250 mg/50 mg per kg body weight, i.p.). The brain was then extracted without perfusion and processed as detailed previously^{51,52}. The left hemisphere was snap frozen on CO₂ pellets and stored at -80°C until processed for western blots. The right hemisphere was sectioned coronally (40 μ m) from the frontal pole to the cerebellum, and sections were saved into 5 serial series for histological staining with about 40 sections per series. For each stain/antibody, at least half a series (20 sections), spaced equally apart (400 μ m) were reacted. Staining was performed at room temperature as described previously^{49,50,52}. Briefly, sections were placed in 0.3% H₂O₂ for 15 min to block endogenous peroxidase activity, and then incubated in mouse-on-mouse (MOM) blocking reagent (Vector Laboratories, Burlingame, CA) to block nonspecific binding for 1 h. Following washes in TBS-Tx, the sections were stained with PHF1 (1:2000 dilution of cell culture supernatant) and MC1 (1:100 dilution of cell culture supernatant) tau antibodies (generously provided by Dr. Peter Davies, Albert Einstein College of Medicine, Bronx, NY). Adjacent sections were also stained with 6E10/4G8 (1:2000 dilution of 1 mg/ml stock of each antibody) for A β deposits. To assess glial response, brain sections were stained with 1) rabbit polyclonal antibody against glial fibrillary acidic protein (GFAP) in astrocytes (1:500; Dako, Carpinteria, CA), and 2) Iba1 (10 μ g/mL; Wako, Richmond, VA) to detect microglia. Neurons were stained with cresyl violet using standard procedure as described previously⁵³.

For staining of microhemorrhages, serial coronal sections of experimental and control mouse brains were mounted on gelatin coated slides and stained with Prussian blue working solution as described previously⁵⁴. Briefly, the brain sections were incubated in a mixture of equal volumes of 10% potassium ferrocyanide (K₄Fe(CN)₆ trihydrate) in distilled H₂O and 20% hydrochloric acid (HCl) for 30 min. The sections were subsequently washed with H₂O, counterstained with nuclear fast red solution for 10 min, washed again with H₂O, dehydrated and coverslipped using Depex mounting media (BDH Laboratory Supplies, England).

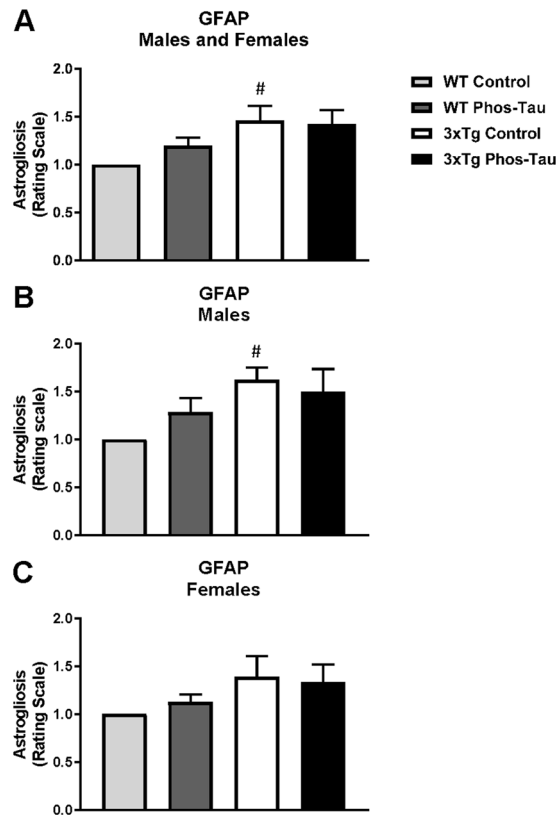


Figure 8. 3xTg mice have more astroglisis than wt mice. (A–C) Semi-quantitative analysis of GFAP immunoreactivity in the subiculum revealed that 3xTg mice had more astroglisis than wt mice ($p = 0.0139$) that was also significantly increased in the males ($p = 0.0286$). However, astroglisis was not significantly affected by the tau immunotherapy in the combined group (A) or in the males (B) and females (C) analyzed separately. * $p < 0.05$ compared to wt control. See text for exact p-values.

Image Analysis. Tau and A β deposition was analyzed in the subiculum of the brain because of its prominent and consistent such pathology. Tau pathology was quantified blindly in 5 sections per brain spaced 200 μm apart similar to as described previously^{5,7,8}. The measurement was the percentage of area in the measurement field (200X) that was occupied by the reaction product (Image), NIH). A β burden was analyzed as per our standard procedure⁵⁴, using the StereoInvestigator Program (Area Fraction Fractionator; MBF Biosciences, Burlington, VT). The area of the grid was 800 $\mu\text{m}^2 \times 800 \mu\text{m}^2$ and A β burden was measured in one frame per section (640 \times 480 μm^2 each) chosen randomly within the subiculum region, and five sections spaced 200 μm apart were analyzed. The A β burden is defined as the percentage of area in the measurement field (subiculum) that is occupied by the reaction product.

The assessment of the Iba1 (microglia) stained sections was based on a semi-quantitative analysis of microgliosis in the subiculum (0, predominantly resting microglia; 1+, a few ramified and/or phagocytic microglia; 2+, moderate number of ramified/phagocytic microglia; 3+, numerous ramified/phagocytic microglia). The rating of the GFAP sections was based on the complexity of astrocytic branching in the subiculum (1+, resting astrocytes, few processes; 2+, reactive astrocytes, moderate branching; 3+, reactive astrocytes, extensive branching).

The haemorrhage profiles (hemosiderin stain) were counted, and the average number of Prussian blue-positive deposits in the subiculum was calculated for each brain section.

All procedures were performed by an individual blinded to the experimental condition of the study. The accuracy of the findings was verified by two independent observers.

Western Blotting. Brains were weighed and homogenized in modified RIPA buffer (50 mM Tris-HCl, pH 7.4, 150 mM NaCl, 1 mM EDTA, 1 mM NaF, 1 mM Na_3VO_4 , 1 $\mu\text{g}/\text{ml}$ complete protease inhibitor cocktail (Roche) and subjected to a low speed spin (14,000 rpm) to remove the membrane fraction. For sarkosyl extraction, 1% sarkosyl solution was added to 300 μL supernatant for a final concentration of 1% and then incubated for 1 h at 37 $^\circ\text{C}$. Sarkosyl extracted supernatant and supernatant without sarkosyl were then centrifuged at 100,000 $\times g$ for 1 h at 4 $^\circ\text{C}$ in Beckman TL-100 ultracentrifuge, and the high-speed supernatants were collected and used for western blot analysis. Sarkosyl extraction results in dissociation of insoluble proteins including aggregated tau proteins. For the insoluble fraction, the pellet was re-suspended in the same volume of buffer without protease and phosphatase inhibitors, but that contained 1% (v/v) Triton X-100 and 0.25% (w/v) deoxycholate sodium. It was then ultracentrifuged at 50,000 $\times g$ for 30 min to retrieve a detergent extracted supernatant that was analyzed as an insoluble fraction^{17,18}.

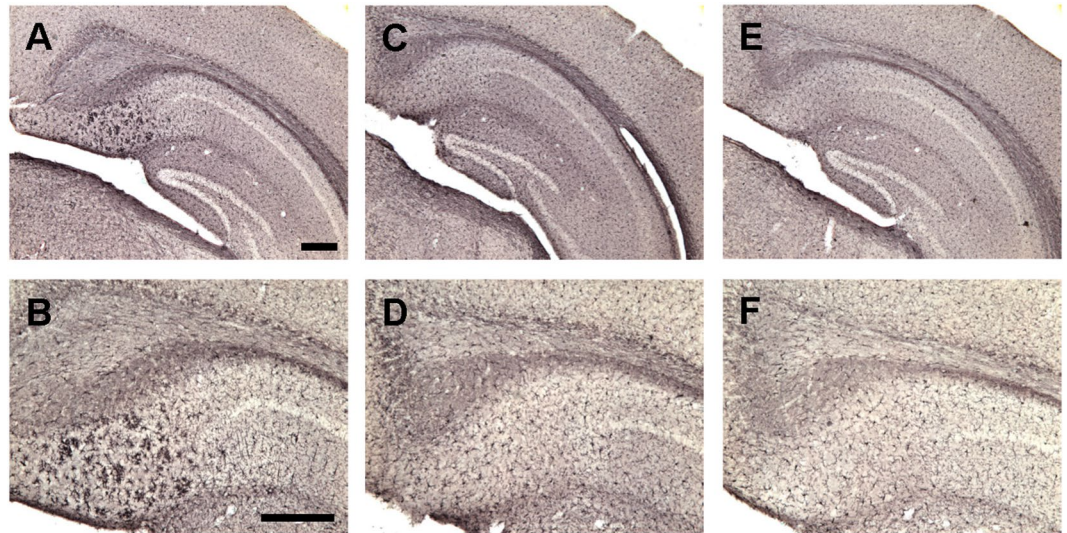


Figure 9. Tau immunization reduces microgliosis in 3xTg mice to wt levels. (A–F) Iba1 immunostaining revealed extensive microgliosis in the subiculum region of the hippocampus in 3xTg mice (A: 5X objective; B: 10X objective) that was greatly reduced in tau immunized mice (C,D) rendering these animals indistinguishable from wt mice (E,F). Scale bar: 250 μ m.

The supernatants from these three fractions were heated at 100 °C for 5 min and the same amount of protein was electrophoresed on a 12% (w/v) polyacrylamide gel. The proteins were then transferred to a nitrocellulose membrane that was subsequently blocked in 5% nonfat milk with 0.1% Tween-20 in TBS, and incubated with different antibodies for at least 3 h at room temperature or at 4 °C overnight (PHF1, CP27 generously provided by Peter Davies). Following washes, the membranes were then incubated for 2 h with 1:2000 horseradish-peroxidase (HRP) conjugated goat anti-mouse antibody (Pierce), developed in ECL (Pierce), imaged with Fuji LAS-4000, and the signal quantified with Multigauge.

Experimental Design and Statistical Analyses. The experimental design was as detailed above. Briefly, transgenic and wt mice of both sexes received short-term prophylactic active tau vaccination at a young age (3–6 months). Control mice received only adjuvant. The mice were bled periodically to determine their antibody titers and they went through behavioral testing at the end of the study (20–22 months). Subsequently, their brains were removed for histological and biochemical analyses of the effects of the vaccination on AD related pathologies, and to monitor potential adverse effects.

All data were analyzed with GraphPad Prism 7. Unless specified below, the analysis was performed with an unpaired t-test, two-tailed. Welch correction was used if the data failed a test of equal variance. When the data failed at least two of three normality tests (Kolmogorov–Smirnov, D’Agostino and Pearson omnibus, and Shapiro–Wilk normality tests), nonparametric Mann–Whitney test was used. That test was also used for analyzing the astro- and microgliosis. Behavioral data was analyzed with one or two-way ANOVA, depending on the number of factors. When the data failed at least two of three normality tests (Kolmogorov–Smirnov, D’Agostino and Pearson omnibus, and Shapiro–Wilk normality tests), nonparametric Kruskal Wallis test was used. Radial arm maze test was analyzed with two-way ANOVA, repeated measures.

Results

Tau immunization elicits a robust antibody response. Mice immunized with the Tau 379–408[P-Ser396, 404] immunogen in Adju-Phos adjuvant developed a robust IgG response in both male and female 3xTg as well as wt mice compared to controls that received adjuvant alone. (Fig. 1A–C). IgM response was less pronounced in the same groups (Fig. 1D–F). Notably, the mice maintained high antibody levels, after the fourth and last immunization at 6 months of age, until the end of the study when the mice were 22 months of age. This was evident both in Tg and wt mice. Plasma from a high titer mouse stained intraneuronal tau aggregates, whereas plasma from a control mouse did not (Fig. 1G,H), which confirms our previous findings that polyclonal antibodies elicited to this vaccine recognize pathological tau protein^{5,10}. In a pilot study, we noticed substantial mortality in the immunized mice after the 5th immunization, with surviving mice maintaining high antibody titer for more than a year. Hence, the enrolled mice received only four vaccine injections. That short vaccination paradigm did not appear to elicit side effects. As noted in Table 1, only a few mice died in three of the groups and none in the immunized 3xTg mice. Based on prior work with this vaccine in other mouse models, the mortality in the pilot study is likely related to more robust immune response to this vaccine in mice on this particular mixed strain background.

Cognitive benefits cannot be detected with the immunotherapy as the Tg mice are not impaired compared to wt mice. The tau immunotherapy did not lead to any significant cognitive improvement in the immunized 3xTg mice, compared to adjuvant treated controls (data not shown). Our analysis however, did

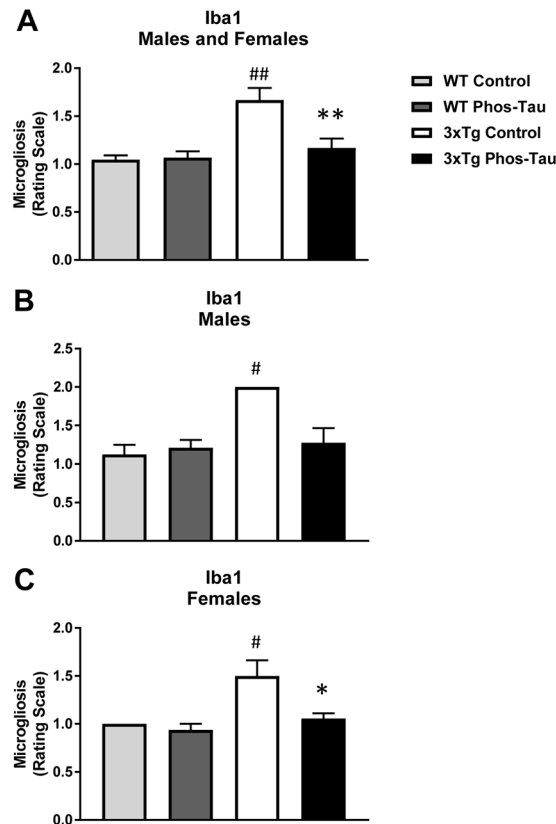


Figure 10. Tau immunization reduces microgliosis in 3xTg mice to wt levels. (A–C) Semi-quantitative analysis of Iba1 immunoreactivity in the subiculum revealed that 3xTg mice had more microgliosis than wt mice (males and females: $p = 0.0013$; males: $p = 0.0286$; females: $p = 0.0310$), and the tau immunotherapy reduced microgliosis in 3xTg mice to wt levels (males and females: $p = 0.0056$; males: $p = 0.0699$; females: $p = 0.0294$). # $p < 0.05$; ## $p < 0.01$ compared to wt control. * $p < 0.05$; ** $p < 0.01$ compared to 3xTg control. See text for exact p-values.

not detect cognitive impairments in the 3xTg controls compared to wt controls. Hence no therapeutic behavioral benefits were observed with the immunotherapy as the mice were not impaired. We have used these same tests extensively in other tangle models^{5,7,8,34}, and observed that Tg tau immunized mice performed better than the Tg control mice. These prior studies include the use of the same tau immunogen. The immunized 3xTg mice and wt mice did not differ significantly from their non-immunized identical control mice in any of the cognitive tasks, and all the groups appeared to have normal motor functions based on our experience with wt mice in these tests (data not shown).

Tau immunization decreases tau pathology. To determine the consequences of the active tau immunization on hyperphosphorylated tau and pathological tau conformers, brain sections were stained with PHF1 and MC1 antibody, respectively. Pronounced tau pathology was revealed with both antibodies, primarily in the subiculum/CA1 region, which was therefore the focus of analysis (Figs 2 and 3A–D). Only background staining was seen in the wt mice (Figs 2 and 3E–H). It may relate to their old age and because the mice were not perfused. The therapy reduced PHF1-reactive tau aggregates by 74% in the combined 3xTg male and female group (Fig. 2I, $p = 0.0008$), which was also significantly reduced in males (Fig. 2J; 68%; $p = 0.0437$) and females (Fig. 2K, 78%; $p = 0.0120$), compared to identical controls. MC1 immunoreactive tau aggregates were also reduced in the immunized 3xTg male and female combined group (Fig. 3I, 70%, $p = 0.0057$), and in the separate female group (Fig. 3K, 86%; $p = 0.0070$), compared to identical controls.

Likewise, western blot analysis revealed a similar clearance of tau in the immunized 3xTg mice. Significant reductions were observed in soluble and insoluble human tau (CP27) in the immunized overall group (Fig. 4A,B, soluble tau: 41%, $p = 0.0103$; insoluble tau: 47%, $p = 0.0008$), and in males (Fig. 4C,D, soluble tau: 38%, $p = 0.0322$; insoluble tau: 47%, $p = 0.0165$), and females (Fig. 4E,F, soluble tau: 48%, $p = 0.0616$; insoluble tau: 49%, $p = 0.0477$), analyzed separately compared to Tg controls. For PHF1 reactive phospho-tau, significant reductions were detected in the insoluble tau fraction in the immunized combined group (Fig. 5B, 42%, $p = 0.0003$), and in males in soluble (Fig. 5C, 76%, $p = 0.0001$) and insoluble tau (Fig. 5D, 58%, $p = 0.0018$). The immunization did not affect endogenous tau in the wt mice (Tau-5: wt controls = $456,740 \pm 76,011$ AUC/mm² (average \pm SEM); wt immunized = $376,469 \pm 98,775$ AUC/mm²).

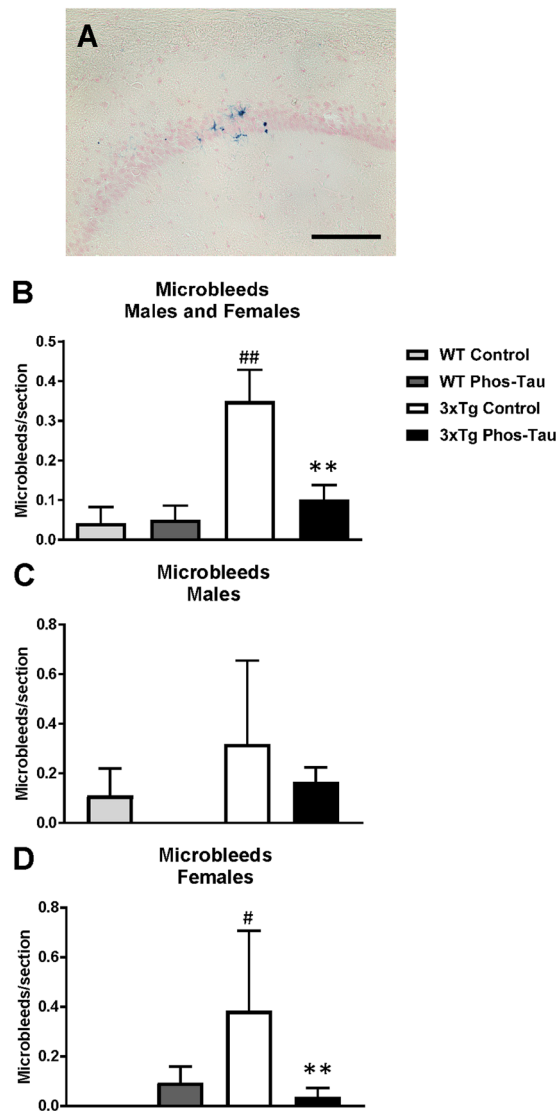


Figure 11. Tau immunization diminishes microbleeds in 3xTg mice to wt levels. (A–D) A few microbleeds (blue) were primarily detected in the hippocampus (A: 20X objective) of the 3xTg control mice (males and females: $p = 0.0088$ compared to wt control; females: $p = 0.0165$), and their numbers were significantly reduced in the tau immunized 3xTg mice (males and females: $p = 0.0095$; females: $p = 0.0078$) to wt levels. Scale bar: 125 μm . # $p < 0.05$; ## $p < 0.01$ compared to wt control. ** $p < 0.01$ compared to 3xTg control. See text for exact p-values.

Tau immunization reduces A β plaque burden. A β plaque burden in the subiculum region of the 3xTg mice was analyzed by immunohistochemistry using a combination of 6E10 and 4G8 antibodies (Fig. 6A–D). Only background staining was seen in the wt mice (Fig. 6E–H). A β deposits in tau immunized 3xTg mice were decreased significantly as compared to control vaccinated mice (Fig. 6I–K, 84% in combined group, $p < 0.0001$; 61% in males, $p = 0.0033$, and; 97% in females, $p < 0.0001$). These results indicate that prophylactic tau immunization reduces the formation of A β plaque deposits.

Tau immunization does not appear to affect neuronal density. Like many other AD models, 3xTg mice do not have extensive neuronal loss^{41,55}. We stained brain sections with cresyl violet from Tg mice that had a robust therapeutic response to the vaccine, and compared those to sections from adjuvant control 3xTg mice. Neuronal density/numbers appeared to be similar in these two groups (data not shown), which fits with the previously reported limited effect of tau or A β pathology on this parameter in this model^{41,55}.

Tau immunization reduces microgliosis and microbleeds but does not affect astrocytes. To assess the potential involvement of activated astrocytes, microglia and microhemorrhage following immunization, histological analysis was performed focusing on the subiculum of the hippocampus, the region with the highest A β plaque burden and associated tauopathy. GFAP immunoreactivity was greater in 3xTg mice compared

to wt mice (males and females: $p = 0.0139$; males: $p = 0.0286$; females: 0.2286) but the immunotherapy did not affect astrogliosis (Figs 7 and 8). Likewise, microgliosis was more pronounced in 3xTg mice than in wt mice (males and females: $p = 0.0013$; males: $p = 0.0699$; females: 0.0294) but the immunotherapy reduced it significantly in the Tg mice (males and females: $p = 0.0056$; males: $p = 0.0699$; females: $p = 0.0294$, Figs 9 and 10). For microhemorrhages, those were also seen more often in 3xTg mice compared to wt mice (males and females: $p = 0.0088$; males: $p = 0.5714$; females: $p = 0.0165$), and were reduced significantly in the treated Tg mice compared to their Tg controls (males and females: $p = 0.0113$; males: $p = 0.4725$; females: $p = 0.0078$, Fig. 11). These results suggest that gradual removal of tau aggregates, and an indirect clearance of A β deposits, are not associated with extensive gliosis or microhemorrhages, and actually reduce microgliosis and microhemorrhages. This lack of treatment associated gliosis is in accordance with our prior results with this immunogen or tau antibody in other tauopathy models^{5,7,8}. Overall, these results support the view that A β and tau pathologies are synergistic. Clearing tau leads indirectly to clearance of A β and associated pathologies such as microgliosis and microhemorrhages.

Discussion

Our findings indicate that tau immunotherapy can not only lead to clearance of tau pathology but also of A β deposits. Importantly as well, the benefits are sustained, lasting at least 16 months following the last immunization. Together, these findings may have major implications for clinical use of this approach. A β immunotherapy has previously been shown to reduce tau pathology to a modest extent in mouse models and humans (reviewed in⁴). Also, a single intrahippocampal injection of a tau antibody reduces early and late tau pathology in 3xTg mice without affecting A β deposits⁴³. In that particular study, clearance of tau pathology was acute and transient, observed at 7 and 14 days post-injection but was no longer evident 21 days after antibody administration. It is, therefore, not surprising that A β pathology was not affected within such a short timeframe. More recently, tau passive immunization was shown to inhibit not only tau but also A β pathology in 3xTg mice that received 6 weekly tau antibody injections at the early stages (12 months) of tau pathology in this model⁴⁴. In our study, the mice received their first vaccine injection at 3 months, and the last one at 6 months, at which age the mice have minimal if any tau or A β pathology. The tau antibodies elicited by the vaccine then prophylactically prevented the development of intraneuronal tau aggregates, which then indirectly attenuated A β deposition. Further support for the synergistic effects of these two pathologies can be obtained from their regional colocalization in the 3xTg model. The A β deposits are most prominent in the subiculum region of the hippocampus and are surrounded by dystrophic neurites positive for pathological tau protein. It can be inferred that neurons with tau lesions generate more A β than healthy neurons that is then deposited near their synaptic terminals. This scenario would then further promote tau pathology and enhanced A β deposition resulting in a vicious cycle. Long-term antibody-mediated removal of tau aggregates would therefore be expected to attenuate the progression of the intertwined tau and A β pathologies as confirmed by our findings.

The tau immunotherapy reduced tau and A β burden in both sexes but the therapeutic benefits were generally more pronounced in females, although they have more pronounced pathology, which fits our prior findings in a different tauopathy model⁷. Associated pathology, microgliosis and microbleeds were also reduced more significantly in females than males following the immunotherapy, which would be expected as these are closely linked to A β deposits.

Cognitive impairment has been previously documented in 3xTg mice (for review see⁵⁶). We were not able to detect such impairments in two different cognitive tests compared to age-matched littermate wt mice. The performance of the wt controls in this study was comparable to our prior reports using these tasks in wt controls of a different strain background but of a similar age^{50,54}. This further supports lack of cognitive deficits of the 3xTg mice in these tasks. However, studies reporting memory issues in this model used different tests. Also, the 3xTg mice we used may have had less severe pathology than in reported studies. Finally, the mice in our study were older than in the prior report. It is conceivable that age-related memory deficits in wt mice may catch up with Tg deficits at the 21–22 months of age when our mice were tested. We are not aware of other reports assessing cognition in this model in mice older than 15–18 months of age⁵⁶. Most of these studies report deficits at various ages ranging from 3–5 months to 15–18 months with a few showing no impairment compared to controls at 1–2 months, 3–5 months and 9–11 months. None of the tests in the prior studies were similar to ours, which further complicates comparison.

Regardless of the lack of a pronounced behavioral phenotype in the 3xTg mice compared to wt mice of the same strain background, the histological effects of the tau immunotherapy were pronounced and highly significant. These findings suggest that prevention of the development of tau pathology can robustly diminish associated A β deposition in mice that are prone to develop such deposits because of APP and PS1 mutations. Remarkably, the therapeutic benefits of the prophylactic immunization were long-lasting, up to 16 months after the fourth and last immunization. Prior active tau immunization studies have not assessed such sustained benefits following the vaccination paradigm. Typically, the final immunization in those studies has been within a month prior to brain analysis. What led us down the path of determining possible long-term benefits of active tau immunization was the unexpected high mortality in this model following the fifth immunization in a pilot study that preceded this comprehensive study. Such catastrophic adverse effects most likely relate to the strong immune response in this particular hybrid strain because 3xTg and wt mice on the same strain background were affected to a similar extent. In our prior studies using this tau immunogen and the same alum adjuvant, we did not observe adverse reactions let alone death in two different tauopathy mouse models that received five or more immunizations^{5,7}. Here, the four immunizations did not appear to lead to side effects. All the 3xTg immunized mice survived until the end of the study, and in each of the other three groups (3xTg and wt controls as well as wt immunized) only a few mice died during the long experimental period (Table 1).

The immunization did not affect tau levels in wt mice. This is as expected because of the phospho-tau immunogen whose epitope is primarily found in pathological tau. Also, the normal tau in wt mice is primarily cytosolic, whereas tau antibodies within neurons typically bind to pathological tau in endosomal-lysosomal vesicles^{10,17,18,21,34,57}.

It remains to be seen if such prolonged prophylactic benefits, not only for blocking tau pathology but also for diminishing A β burden, will hold up in humans receiving active tau immunizations. It is unlikely that this will be clarified in ongoing active tau immunization trials as the enrolled subjects are likely to have already substantial A β deposits, whose development may have plateaued because of synaptic loss. As in our study, prophylactic therapy will likely be required, which could be assessed first in individuals with genetic mutations that are known to cause AD or related tauopathies. However, because the extent of tau pathology correlates much better with cognitive deficits than A β burden, tau immunotherapies are likely to provide clinical benefits at later stages of AD than treatments that directly target A β .

References

- Grundke-Iqbal, I. *et al.* Abnormal phosphorylation of the microtubule-associated protein tau (tau) in Alzheimer cytoskeletal pathology. *Proc. Natl. Acad. Sci. USA* **83**, 4913–4917 (1986).
- Selkoe, D. J. & Hardy, J. The amyloid hypothesis of Alzheimer's disease at 25 years. *EMBO Mol. Med.* **8**, 595–608 (2016).
- Braak, H., Thal, D. R., Ghebremedhin, E. & Del, T. K. Stages of the pathologic process in Alzheimer disease: age categories from 1 to 100 years. *J. Neuropathol. Exp. Neurol.* **70**, 960–969 (2011).
- Congdon, E. E., Krishnaswamy, S. & Sigurdsson, E. M. Harnessing the immune system for treatment and detection of tau pathology. *J. Alzheimers. Dis.* **40**, S113–S121 (2014).
- Asuni, A. A., Boutajangout, A., Quartermain, D. & Sigurdsson, E. M. Immunotherapy targeting pathological tau conformers in a tangle mouse model reduces brain pathology with associated functional improvements. *J. Neurosci.* **27**, 9115–9129 (2007).
- Boimel, M. *et al.* Efficacy and safety of immunization with phosphorylated tau against neurofibrillary tangles in mice. *Exp. Neurol.* **224**, 472–485 (2010).
- Boutajangout, A., Quartermain, D. & Sigurdsson, E. M. Immunotherapy targeting pathological tau prevents cognitive decline in a new tangle mouse model. *J. Neurosci.* **30**, 16559–16566 (2010).
- Boutajangout, A., Ingadottir, J., Davies, P. & Sigurdsson, E. M. Passive immunization targeting pathological phospho-tau protein in a mouse model reduces functional decline and clears tau aggregates from the brain. *J. Neurochem.* **118**, 658–667 (2011).
- Chai, X. *et al.* Passive immunization with anti-Tau antibodies in two transgenic models: reduction of Tau pathology and delay of disease progression. *J. Biol. Chem.* **286**, 34457–34467 (2011).
- Krishnamurthy, P. K., Deng, Y. & Sigurdsson, E. M. Mechanistic Studies of Antibody-Mediated Clearance of Tau Aggregates Using an *ex vivo* Brain Slice Model. *Front Psychiatry* **2**, 59–65 (2011).
- Bi, M., Ittner, A., Ke, Y. D., Gotz, J. & Ittner, L. M. Tau-Targeted Immunization Impedes Progression of Neurofibrillary Histopathology in Aged P301L Tau Transgenic Mice. *PLoS. One.* **6**, e26860 (2011).
- Troquier, L. *et al.* Targeting phospho-Ser422 by active Tau immunotherapy in the THY-Tau22 mouse model: a suitable therapeutic approach. *Curr. Alzheimer Res.* **9**, 397–405 (2012).
- Kfoury, N., Holmes, B. B., Jiang, H., Holtzman, D. M. & Diamond, M. I. Trans-cellular Propagation of Tau Aggregation by Fibrillar Species. *J. Biol. Chem.* **287**, 19440–19451 (2012).
- d'Abramo, C., Acker, C. M., Jimenez, H. T. & Davies, P. Tau Passive Immunotherapy in Mutant P301L Mice: Antibody Affinity versus Specificity. *PLoS ONE* **8**, e62402 (2013).
- Theunis, C. *et al.* Efficacy and safety of a liposome-based vaccine against protein Tau, assessed in tau P301L mice that model tauopathy. *PLoS. One.* **8**, e72301 (2013).
- Yanamandra, K. *et al.* Anti-tau antibodies that block tau aggregate seeding *in vitro* markedly decrease pathology and improve cognition *in vivo*. *Neuron* **80**, 402–414 (2013).
- Gu, J., Congdon, E. E. & Sigurdsson, E. M. Two novel Tau antibodies targeting the 396/404 region are primarily taken up by neurons and reduce Tau protein pathology. *J. Biol. Chem.* **288**, 33081–33095 (2013).
- Congdon, E. E., Gu, J., Sait, H. B. & Sigurdsson, E. M. Antibody Uptake into Neurons Occurs Primarily via Clathrin-dependent Fc γ Receptor Endocytosis and Is a Prerequisite for Acute Tau Protein Clearance. *J. Biol. Chem.* **288**, 35452–35465 (2013).
- Castillo-Carranza, D. L. *et al.* Specific targeting of tau oligomers in htau mice prevents cognitive impairment and tau toxicity following injection with brain-derived tau oligomeric seeds. *J. Alzheimers. Dis.* **40**, S97–S111 (2014).
- Castillo-Carranza, D. L. *et al.* Passive Immunization with Tau Oligomer Monoclonal Antibody Reverses Tauopathy Phenotypes without Affecting Hyperphosphorylated Neurofibrillary Tangles. *J. Neurosci.* **34**, 4260–4272 (2014).
- Collin, L. *et al.* Neuronal uptake of tau/pS422 antibody and reduced progression of tau pathology in a mouse model of Alzheimer's disease. *Brain* **137**, 2834–2846 (2014).
- Ittner, A. *et al.* Tau-targeting passive immunization modulates aspects of pathology in tau transgenic mice. *J. Neurochem.* **132**, 135–145 (2015).
- Kontsekova, E., Zilka, N., Kovacech, B., Novak, P. & Novak, M. First-in-man tau vaccine targeting structural determinants essential for pathological tau-tau interaction reduces tau oligomerisation and neurofibrillary degeneration in an Alzheimer's disease model. *Alzheimers. Res. Ther.* **6**, 44 (2014).
- Selenica, M. L. *et al.* Epitope analysis following active immunization with tau proteins reveals immunogens implicated in tau pathogenesis. *J. Neuroinflammation.* **11**, 152 (2014).
- Ando, K. *et al.* Vaccination with Sarkosyl insoluble PHF-tau decrease neurofibrillary tangles formation in aged tau transgenic mouse model: a pilot study. *J. Alzheimers. Dis.* **40**(Suppl 1), S135–S145 (2014).
- Castillo-Carranza, D. L. *et al.* Specific targeting of tau oligomers in Htau mice prevents cognitive impairment and tau toxicity following injection with brain-derived tau oligomeric seeds. *J. Alzheimers. Dis.* **40**(Suppl 1), S97–S111 (2014).
- Umeda, T. *et al.* Passive immunotherapy of tauopathy targeting pSer413-tau: a pilot study in mice. *Ann. Clin. Transl. Neurol.* **2**, 241–255 (2015).
- Sankaranarayanan, S. *et al.* Passive immunization with phospho-tau antibodies reduces tau pathology and functional deficits in two distinct mouse tauopathy models. *PLoS. One.* **10**, e0125614 (2015).
- Yanamandra, K. *et al.* Anti-tau antibody reduces insoluble tau and decreases brain atrophy. *Ann. Clin. Transl. Neurol.* **2**, 278–288 (2015).
- d'Abramo, C., Acker, C. M., Jimenez, H. & Davies, P. Passive Immunization in JNPL3 Transgenic Mice Using an Array of Phospho-Tau Specific Antibodies. *PLoS. One.* **10**, e0135774 (2015).
- Luo, W. *et al.* Microglial internalization and degradation of pathological tau is enhanced by an anti-tau monoclonal antibody. *Sci. Rep.* **5**, 11161 (2015).
- Funk, K. E., Mirbaha, H., Jiang, H., Holtzman, D. M. & Diamond, M. I. Distinct Therapeutic Mechanisms of Tau Antibodies: Promoting Microglial Clearance Versus Blocking Neuronal Uptake. *J. Biol. Chem.* **290**, 21652–21662 (2015).

33. Schroeder, S. K., Joly-Amado, A., Gordon, M. N. & Morgan, D. Tau-Directed Immunotherapy: A Promising Strategy for Treating Alzheimer's Disease and Other Tauopathies. *J. Neuroimmune Pharmacol.* **11**, 9–25 (2016).
34. Congdon, E. E. *et al.* Affinity of Tau antibodies for solubilized pathological Tau species but not their immunogen or insoluble Tau aggregates predicts *in vivo* and *ex vivo* efficacy. *Mol. Neurodegener.* **11**, 62–85 (2016).
35. Liu, W. *et al.* Vectored Intracerebral Immunization with the Anti-Tau Monoclonal Antibody PHF1 Markedly Reduces Tau Pathology in Mutant Tau Transgenic Mice. *J. Neurosci.* **36**, 12425–12435 (2016).
36. Pedersen, J. T. & Sigurdsson, E. M. Tau immunotherapy for Alzheimer's disease. *Trends Mol. Med.* **21**, 394–402 (2015).
37. Castillo-Carranza, D. L. *et al.* Tau immunotherapy modulates both pathological tau and upstream amyloid pathology in an Alzheimer's disease mouse model. *J. Neurosci.* **35**, 4857–4868 (2015).
38. Mably, A. J. *et al.* Tau immunization: a cautionary tale? *Neurobiol. Aging* **36**, 1316–1332 (2015).
39. Rosenmann, H. *et al.* Tauopathy-like abnormalities and neurologic deficits in mice immunized with neuronal tau protein. *Archives of Neurology* **63**, 1459–1467 (2006).
40. Rozenstein-Tsalkovich, L. *et al.* Repeated immunization of mice with phosphorylated-tau peptides causes neuroinflammation. *Exp. Neurol.* **248**, 451–456 (2013).
41. Oddo, S. *et al.* Triple-transgenic model of Alzheimer's disease with plaques and tangles: Intracellular A β and synaptic dysfunction. *Neuron* **39**, 409–421 (2003).
42. Oddo, S., Billings, L., Kesslak, J. P., Cribbs, D. H. & LaFerla, F. M. A β immunotherapy leads to clearance of early, but not late, hyperphosphorylated tau aggregates via the proteasome. *Neuron* **43**, 321–332 (2004).
43. Walls, K. C. *et al.* p-Tau immunotherapy reduces soluble and insoluble tau in aged 3xTg-AD mice. *Neurosci. Lett.* **575**, 96–100 (2014).
44. Dai, C. L., Tung, Y. C., Liu, F., Gong, C. X. & Iqbal, K. Tau passive immunization inhibits not only tau but also A β pathology. *Alzheimers. Res. Ther.* **9**, 1 (2017).
45. Boutajangout, A., Li, Y. S., Quartermain, D. & Sigurdsson, E. M. Cognitive and sensorimotor tasks for assessing functional impairments in mouse models of Alzheimer's disease and related disorders. *Methods Mol Biol* **849**, 529–540 (2012).
46. Davenport, J. W., Hagquist, W. W. & Rankin, G. R. Symmetrical Maze - An Automated Closed-Field Test Series for Rats. *Behavior Research Methods & Instrumentation* **2**, 112–118 (1970).
47. Hebb, D. O. & Williams, K. A. A method of rating animal intelligence. *J. Gen. Psychol.* **34**, 59–65 (1946).
48. Rabinovitch, M. S. & Rosvold, H. E. A closed-field intelligence test for rats. *Can. J. Psychol.* **5**, 122–128 (1951).
49. Sigurdsson, E. M., Scholtzova, H., Mehta, P. D., Frangione, B. & Wisniewski, T. Immunization with a non-toxic/non-fibrillar amyloid- β homologous peptide reduces Alzheimer's disease associated pathology in transgenic mice. *Am. J. Pathol.* **159**, 439–447 (2001).
50. Sigurdsson, E. M. *et al.* An attenuated immune response is sufficient to enhance cognition in an Alzheimer's disease mouse model immunized with amyloid- β derivatives. *J. Neurosci.* **24**, 6277–6282 (2004).
51. Sigurdsson, E. M., Lorens, S. A., Hejna, M. J., Dong, X. W. & Lee, J. M. Local and distant histopathological effects of unilateral amyloid- β 25–35 injections into the amygdala of young F344 rats. *Neurobiol. Aging* **17**, 893–901 (1996).
52. Rajamohamedsait, H. B. & Sigurdsson, E. M. Histological Staining of Amyloid and Pre-amyloid Peptides and Proteins in Mouse Tissue. *Methods Mol Biol* **849**, 411–424 (2012).
53. Sigurdsson, E. M., Lee, J. M., Dong, X. W., Hejna, M. J. & Lorens, S. A. Bilateral injections of amyloid- β 25–35 into the amygdala of young Fischer rats: Behavioral, neurochemical, and time dependent histopathological effects. *Neurobiology of Aging* **18**, 591–608 (1997).
54. Asuni, A. A. *et al.* Vaccination of Alzheimer's model mice with A β derivative in alum adjuvant reduces A β burden without microhemorrhages. *Eur. J. Neurosci.* **24**, 2530–2542 (2006).
55. Billings, L. M., Oddo, S., Green, K. N., McGaugh, J. L. & LaFerla, F. M. Intra-neuronal A β causes the onset of early Alzheimer's disease-related cognitive deficits in transgenic mice. *Neuron* **45**, 675–688 (2005).
56. Webster, S. J., Bachstetter, A. D., Nelson, P. T., Schmitt, F. A. & Van Eldik, L. J. Using mice to model Alzheimer's dementia: an overview of the clinical disease and the preclinical behavioral changes in 10 mouse models. *Front. Genet.* **5**, 88 (2014).
57. Krishnaswamy, S. *et al.* Antibody-derived *in vivo* imaging of tau pathology. *J. Neurosci.* **34**, 16835–16850 (2014).

Acknowledgements

EMS was supported by NIH R01 grants NS077239, AG032611 and AG020197 and in part by R24OD18340 and R24OD018339 during these experiments. We thank Frank LaFerla and Salvatore Oddo for providing breeding pairs of the 3xTg and wt mice, and Peter Davies for the tau antibodies, CP27, PHF1 and MCI.

Author Contributions

E.M.S. designed the experiments, analyzed the data and wrote the paper; H.R. performed the immunizations, antibody measurements, behavioral analysis, brain sectioning and immunohistochemistry. S.R. performed the western blots and related analysis, and participated in the histological analysis. W.R. assisted H.R. and S.R. Y.L. performed immunohistochemistry, western blots and related analyses.

Additional Information

Supplementary information accompanies this paper at <https://doi.org/10.1038/s41598-017-17313-1>.

Competing Interests: E.M.S. is an inventor on patents on tau immunotherapy and related diagnostics that are assigned to New York University. This technology is licensed to and is being co-developed with H. Lundbeck A/S.

Publisher's note: Springer Nature remains neutral with regard to jurisdictional claims in published maps and institutional affiliations.



Open Access This article is licensed under a Creative Commons Attribution 4.0 International License, which permits use, sharing, adaptation, distribution and reproduction in any medium or format, as long as you give appropriate credit to the original author(s) and the source, provide a link to the Creative Commons license, and indicate if changes were made. The images or other third party material in this article are included in the article's Creative Commons license, unless indicated otherwise in a credit line to the material. If material is not included in the article's Creative Commons license and your intended use is not permitted by statutory regulation or exceeds the permitted use, you will need to obtain permission directly from the copyright holder. To view a copy of this license, visit <http://creativecommons.org/licenses/by/4.0/>.